Endocrine Journal

ORIGINAL

Advance Publication
doi:10.1507/endocrj.EJ18-0387

Characterization of a novel *CDC73* gene mutation in a hyperparathyrodism-jaw tumor patient affected by parathyroid carcinoma in the absence of somatic loss of heterozygosity

Simone Ciuffi[1)], Luisella Cianferotti[2)], Gabriella Nesi[3)], Ettore Luzi[1)], Francesca Marini[1)], Francesca Giusti[2)], Roberto Zonefrati[1)], Giorgio Gronchi[1)], Giuliano Perigli[4)] and Maria Luisa Brandi[2)]

[1)] *Department of Surgery and Translational Medicine, University of Florence, Florence 50139, Italy*
[2)] *Department of Surgery and Translational Medicine, University of Florence, Unit of Bone and Mineral Diseases, University Hospital of Florence, Florence 50139, Italy*
[3)] *Department of Surgery and Translational Medicine, University of Florence, Section of Pathological Anatomy, University Hospital of Florence, Florence 50139, Italy*
[4)] *Department of Surgery and Translational Medicine, University of Florence, Unit of General Surgery, University Hospital of Florence, Florence 50139, Italy*

Abstract. Hyperparathyrodism-jaw tumor (HPT-JT) syndrome is an autosomal dominant disorder. Loss of function of the cell division cycle protein 73 homolog (*CDC73*) gene is responsible for the syndrome. This gene encodes an ubiquitously expressed 531 amino acid protein, parafibromin, that acts as a tumor suppressor. Loss of heterozygosity (LOH) of the *CDC73* locus in many HPT-JT associated parathyroid tumors from patients with germline mutation is in accordance with Knudson's "two-hit" model for hereditary cancer. A 41-year-old man with mandible ossifying fibroma suffered from severe hypercalcemia due to parathyroid carcinoma (PC). Genetic analysis was performed to evaluate germinal and somatic *CDC73* gene mutation as well as real-time qRT-PCR to quantify *CDC73* mRNA, miR-155 and miR-664 expression levels. Immunohistochemistry and Western blotting (WB) assay were carried out to evaluate parafibromin protein expression. A novel heterozygous nonsense mutation, c.191-192 delT, was identified in the *CDC73* gene. No *CDC73* LOH was found in PC tissue, nor any differences in expression levels for *CDC73* gene, miR-155 and miR-664 between PC and parathyroid adenoma control tissues. On the contrary, both immunohistochemistry and WB assay showed an approximate 90% reduction of parafibromin protein expression in PC. In conclusion, this study describes a novel germinal mutation, c.191-192 delT, in the *CDC73* gene. Despite normal *CDC73* gene expression, we found a significant decrease in parafibromin. We hypothesize that a gene silencing mechanism, possibly induced by microRNA, could play a role in determining somatic post-transcriptional inactivation of the wild type *CDC73* allele.

Key words: Hyperparathyrodism-jaw tumor syndrome, *CDC73* gene, Parafibromin, Parathyroid carcinoma, microRNA

HYPERPARATHYROIDISM-JAW TUMOR SYNDROME (HPT-JT) (OMIM phenotype number #145001), is a rare autosomal dominant disorder with incomplete penetrance. This endocrine disease is characterized by primary hyperparathyroidism (PHPT) due to the occurrence of single or multiple parathyroid tumors (PTs). PTs are detectable by hypercalcemia, occur in 95% of HPT-JT patients and are malignant in 15% of cases [1, 2]. In addition, 25–50% of HPT-JT patients may develop ossifying fibroma of maxilla/mandible (OFM) [3, 4] as well as uterine and renal tumors [5].

HPT-JT syndrome ensues from inactivating germline

Submitted Oct. 4, 2018; Accepted Jan. 17, 2019 as EJ18-0387
Released online in J-STAGE as advance publication Feb. 22, 2019
Correspondence to: Maria Luisa Brandi, MD, PhD, Full Professor of Endocrinology, Unit of Bone and Mineral Metabolic Diseases, Department of Surgery and Translational Medicine, University of Florence, Largo Palagi 1-50139 Florence, Italy.
E-mail: marialuisa.brandi@unifi.it

Abbreviations: HPT-JT, hyperparathyrodism-jaw tumor; PHPT, primary hyperparathyroidism; PT, parathyroid tumors; OFM, ossifying fibroma of maxilla/mandible; CDC73, cell division cycle protein 73 homolog; HRPT2, hyperparathyroidism type 2; LOH, loss of heterozygosity; PC, parathyroid carcinoma; IHC, immunohistochemistry; miRs, microRNAs; FFPE, formalin-fixed paraffin-embedded; PAs, parathyroid adenomas; PBL, peripheral blood leukocytes; DAB, 3,3'-diaminobenzidine; WB, Western blot.

mutation of the cell division cycle protein 73 homolog (*CDC73*) gene (OMIM 607393), previously known as hyperparathyroidism type 2 (*HRPT2*) gene. Indeed, mutations of this gene have been identified in over 80% of the reported HPT-JT families [6]. *CDC73* gene encodes an ubiquitously expressed, evolutionarily conserved 531 amino acid protein, parafibromin, predominantly expressed in the nucleus [7]. This protein acts as a transcriptional regulator as part of a RNA polymerase II associated complex, known as the Polymerase Associated Factor 1 complex [4]. The 60 kDA parafibromin regulates transcriptional and post-transcriptional events [8], WNT and Hedgehog pathway target genes, by β-catenin and Gli proteins binding, respectively [9, 10] and chromatin remodeling [8]. Parafibromin has been considered a tumor suppressor protein, based on its ability to induce apoptosis [11], cell cycle and cell proliferation arrest by repressing Cyclin D1 [12] and MYC expression respectively [13]. Indeed, loss of heterozygosity (LOH) of the *CDC73* locus in HPT-JT associated tumors is consistent with Knudson's 'two hit' model for hereditary cancer [14], confirmed by the fact that over 75% of patients with parathyroid carcinoma (PC) show inactivating *CDC73* somatic/germline mutation [15] with consequent reduced or absent parafibromin immunoreactivity. Mutational screening of the *CDC73* gene and immunohistochemistry (IHC) to evaluate parafibromin expression are therefore two important tests for PC diagnosis, although some reports have shown that the sensitivity and specificity of these tests is insufficient for an accurate diagnosis. However, HPT-JT families and PC patients harboring no *CDC73* gene mutation have also been reported; no phenotypic differences have been observed between clinical manifestations of patients with or without inactivating *CDC73* gene mutation [5]. Modifications in *CDC73* gene function could be ascribed to promoter mutation, large deletions not detectable by PCR/sequence analysis or epigenetic regulation mechanisms resulting in gene silencing, including DNA methylation, histone modifications, or microRNAs expression.

MicroRNAs (miRs), short 19–25 nucleotide endogenously expressed single-strand noncoding RNAs, are negative regulators of gene expression through the increased degradation and/or decreased translation of mRNAs target, without modifying their transcription levels [16, 17]. They account for 1% of the genome and their expression is highly tissue specific. miRs can also act as either tumor suppressors or oncogenes in most carcinomas [18]. Dysregulated expression of miRs in PC has been identified in a limited number of studies [19-22]. When compared with non-malignant PT, miR-222, miR-503, miR-371, miR-372, miR-517c and Cluster C19MC were overexpressed in PC, while miR-139, miR-296, miR-26b, miR-30b and miR-126* were downregulated. However, none of these miRs targeted *CDC73* mRNA. To date, only two studies have identified specific miRs, miR-155 and miR-664, as responsible for downregulation of the *CDC73* gene expression, in oral squamous cell carcinoma [23] and MEN1 parathyroid adenoma [24], respectively.

This study reports the case of an HPT-JT patient with a novel *CDC73* germline gene mutation, who developed PC in the absence of any documented somatic LOH in the *CDC73* gene.

Materials and Methods

Clinical case

A 41-year-old male, who had undergone removal of a mandible ossifying fibroma, presented with severe hypercalcemia (total serum calcium 15 mg/dL), elevated serum intact PTH levels (470 pg/mL) and a high degree of bone demineralization (Bone Mineral Density T-score of –3.6 in the lumbar spine and –4.5 in the distal radius). Ultrasound of the neck suggested a right upper PT (35 × 20 × 10 mm) that was excised under general anesthesia and histologically diagnosed as PC. Hematoxylin-eosin stained sections revealed a hypercellular tumor with a trabecular growth pattern and subdivided by broad bands of fibrous connective tissue. Neoplastic cells exhibited marked pleomorphism with coarsely clumped chromatin and macronucleoli. Mitotic figures with atypical forms were seen. Vascular invasion was also detected in the absence of tissue necrosis. The tumor capsule was intact and surgical margins were negative (Fig. 1). Removal of the PT resulted in severe hungry bone syndrome, which required administration of calcium and active vitamin D metabolites. Consequently, serum calcium and PTH levels had returned within the normal range, respectively 9.4 mg/dL and 11.3 pg/mL.

The patient's father deceased at 62 years due to causes unrelated to HPT-JT syndrome (cause of death: pancreatic cancer). The mother (68 years old) and the sister (38 years old) were referred as healthy at the time of this study. Furthermore, the mother was resulted negative for *CDC73* gene mutation analysis, while the sister refused to undergo through genetic testing.

Genetic test, histology and molecular biology analysis

Peripheral blood, frozen and formalin-fixed paraffin-embedded (FFPE) PC tissue of the patient were collected using standard procedures. Since no normal parathyroid tissue samples were available, three parathyroid adenomas (PAs), not harboring mutations in either *CDC73* or

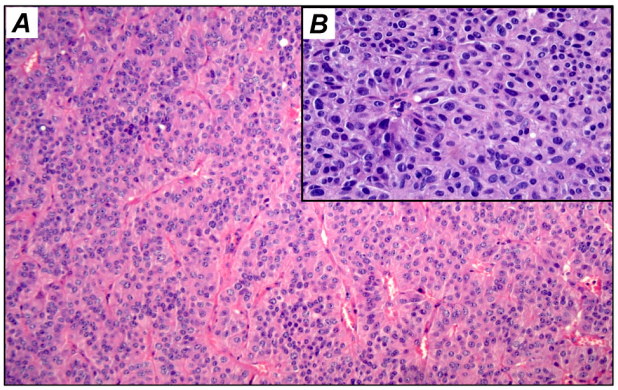

Fig. 1 Histologic appearance of PC by hematoxylin-eosin stain. A, diffuse trabecular growth pattern intersected by broad fibrous bands (40× original magnification). B, chief cells with significant pleomorphism and increased mitotic activity (400× original magnification).

MEN1 genes, were used as controls. PA and PC differ in origin, progression and molecular mechanisms [25], suggesting that PA can be used as control tissue.

DNA was extracted from both peripheral blood leucocytes (PBL) and frozen PC tissue using the MagCore Genomic DNA Whole Blood Kit (RBC Bioscience, Xindian City, Taipei, Taiwan) in an automated extractor system MagCore HF16, and TRIzol Reagent (Invitrogen, Carlsbad, CA, USA), respectively, as recommended by the manufacturers.

Genetic analysis to evaluate germinal and somatic mutations of the whole *CDC73* coding sequence (17 exons, including exon-intron boundaries) was performed by PCR amplification and direct Sanger sequencing on genomic DNA extracted from both PBL and PC frozen tissue. Briefly, PCR reactions were carried out in a 50 µL reaction solution containing 5 µL 10X PCR Buffer (Thermo Scientific, Waltham, Massachusetts, USA), 0.2 nM dNTPs, 10 pmol of each primer, 1.25 U DreamTaq DNA Polymerase (Thermo Scientific, Waltham, Massachusetts, USA) and 50 ng of DNA. PCR cycling conditions consisted of an initial 5 min denaturation step at 95°C, followed by 30 cycles of 95°C for 30 s annealing for 30 s and extension at 72°C for 30 s, with final extension at 72°C for 5 min. Annealing temperatures were optimized for all primer sets (Table 1). Purified PCR products were sequenced using the Big Dye Terminator Cycle Sequencing Kit v. 1.1 (Applied Biosystems, Foster City, CA, USA). Purified sequencing reactions were separated on ABI PRISM 3100xl genetic analyzer capillary sequencer (Applied Biosystems, Foster City, CA, USA).

Total RNA was extracted from the three frozen PA samples using TRIzol Reagent (Invitrogen, Carlsbad, CA, USA) as recommended by the manufacturers. RT-PCR analysis was employed to determine whether the PC tissue had maintained its differentiated endocrine status by evaluating *PTH* gene expression. RT-PCR and real-time qRT-PCR analysis were performed to evaluate the *CDC73* gene expression levels in PC tissue. Table 1 gives primer sets for both *PTH* and *CDC73* gene expression. For RT-PCR analysis, first-strand cDNA was prepared from 1 µg of total RNA, using a QuantiTect Reverse Transcription Kit (QIAGEN, Hilden, Germany) as recommended by the manufacturers. RT-PCR reactions were tested as described above, utilizing 50 ng of cDNA. For real-time qRT-PCR analysis, cDNA was prepared from 50 ng of total DNA-free RNA, using a QuantiTect Reverse Transcription Kit (QIAGEN, Hilden, Germania) as recommended by the manufacturers. Real-time qRT-PCR was performed using a Rotor-Gene Q (QIAGEN, Hilden, Germany). A reaction solution of 20 µL was prepared, containing 10 µL of KAPA SYBR FAST qPCR Master Mix (Kapa Biosystems, Wilmington, MA, USA), 10 pmol of forward and reverse primers and 2.5 ng of cDNA (Table 1). Real-time qRT-PCR conditions were: 95°C for 3 min, followed by 40 cycles of 95°C for 3 s, 62°C for 20 s, and 72°C for 15 s. Relative quantification was calculated through the $2^{-\Delta\Delta ct}$ method, and normalized using *RPS18* mRNA.

IHC was carried out on FFPE PC tissue sections to assess parafibromin expression and Ki-67 proliferative index. Mouse monoclonal anti-parafibromin (clone 2H1, dilution 1:100; Santa Cruz Biotechnology, Santa Cruz, CA, USA) was used as primary antibody. Antigen retrieval was carried out with Epitope Retrieval Solution Citrate buffer (10 mM, pH 6; Dako, Glostrup, Denmark) in a thermostatic bath. Sections were incubated overnight at 4°C. Immunohistochemical analysis was performed using EnVision FLEX Systems (Dako, Glostrup, Denmark) and 3,3'-diaminobenzidine (DAB) (Dako, Glostrup, Denmark) as the chromogen in Dako Autostainer Link48 Instrument (Dako, Glostrup, Denmark). Additional serial sections were stained with rabbit monoclonal anti-Ki-67 (clone 30.9, ready-to-use; Ventana, Tucson, AZ, USA) on a Ventana BenchMark ULTRA immunostainer (Ventana Medical Systems). The Ventana staining procedure included pretreatment with cell conditioner 1 followed by incubation with the antibody. The signal was then developed with ultraView Universal DAB Detection Kit. Positive controls comprised human colon for parafibromin and human skin for Ki-67. Negative controls were performed by substituting the primary antibody with a mouse serum (normal) and rabbit serum (normal) (Dako, Glostrup, Denmark), respectively. The control sections were treated in parallel with the samples. The sections were lightly counterstained with Mayer's hematoxylin and mounted with Permount.

For Western blot (WB) analysis, proteins were extrac-

Table 1 Primers, amplicon sizes, melting temperature and analysis type

Primer name	Sequence (5'-3')	Size (bp)	Tm (°C)	Analysis type
CDC73 Ex1-F	GAGGACGGCTGTTAGTGCT	451	60	Genetic screening
CDC73 Ex1-R	CCCCTTCTTTCCTTACCCTA			
CDC73 Ex2-F	TGTCATTGCCTTCCTTTGTG	400	60	Genetic screening
CDC73 Ex2-R	GATCACACCACTGCACCCTA			
CDC73 Ex3-F	GTTGTGTATCATTGTTATTC	328	56	Genetic screening
CDC73 Ex3-R	GACAGTGCATCCACTGTATAAG			
CDC73 Ex4-F	AACATGTTTTTGCAGAGCTG	451	58	Genetic screening
CDC73 Ex5-R	CTCCTCAGGTTACTGCAATC			
CDC73 Ex6-F	GGCCTAAAGACACTGATACC	351	62	Genetic screening
CDC73 Ex6-R	CGAACTTAAGAGCAAAGAGG			
CDC73 Ex7-F	GAATGCCTGCTGTGAAAA	502	55	Genetic screening
CDC73 Ex7-R	TGTGAAGGAGCTTGCATTT			
CDC73 Ex8-F	GACATATGTAGTAGGGAAG	362	58	Genetic screening
CDC73 Ex8-R	GGGAGGGCTTTCACATCTTT			
CDC73 Ex9-F	ATGGTCATGCTACTGCACTC	251	56	Genetic screening
CDC73 Ex9-R	CCAACCCTTACCCTTAAACA			
CDC73 Ex10-F	ACAATAGGCTTGCTGGTCTG	332	56	Genetic screening
CDC73 Ex10-R	TCCCTGGAACAAAAGAACATC			
CDC73 Ex11-F	CAGTGGAGTAACCAACTGAGTGA	395	60	Genetic screening
CDC73 Ex11-R	GCTGACTGAAGTTTAGCAAGCA			
CDC73 Ex12-F	CAGTGTTGAGAAGATAGTTG	612	56	Genetic screening
CDC73 Ex13-R	GTATCTCAATATCCTACGTACAGG			
CDC73 Ex14-F	ATCTTCCCATTTTCATCACG	321	56	Genetic screening
CDC73 Ex14-R	CCCCATCTCTTAAAAAGCAA			
CDC73 Ex15-F	TGCCTAAGGGATTTATAGTAGC	281	55	Genetic screening
CDC73 Ex15-R	ACATCATATGCGCAGAACT			
CDC73 Ex16-F	ATACGGCTTCAGTTGGTGGA	345	58	Genetic screening
CDC73 Ex16-R	TGTTGAAAGAAGGGAATTAGGG			
CDC73 Ex17-F	GAGGAGTGTTATTTCTAGCTTATTC	341	60	Genetic screening
CDC73 Ex17-R	TCTCCTTGAAGCACAAAGCATCA			
PTH-F	TCACCATTTAAGGGGTCTGC	192	62	RT-PCR
PTH-R	CAGATTTCCCATCCGATTTTG			
CDC73-F	GACCCGAGATATTGTCAGCA	128	62	RT-PCR, qRT-PCR
CDC73-R	GCCCTTCTTCTCTGGCTTTT			
RPS18-F	AAATACAGCCAGGTCCTAGC	190	62	RT-PCR, qRT-PCR
RPS18-R	GCCTACAGACTTATTTCTTCTTGG			

ted from PC and three PAs frozen tissues, using PARIS Kit (Ambion, Thermo Scientific, Waltham, MA, USA) supplemented with a protease inhibitor cocktail. Total protein was quantified with a BCA Protein Assay Kit (Thermo Scientific, Waltham, MA, USA). 30 µg of proteins were loaded on a 10% SDS-PAGE gel and electrotransferred to PVDF membranes (Millipore, Burlington, MA, USA). The membranes were blocked with Odyssey

Blocking Buffer (LI-COR, Lincoln, NE, USA), and incubated overnight at 4°C with rabbit polyclonal anti-parafibromin antibody (A264, Cell Signaling Technology, Danvers, MA, USA) at 1:1,000 dilution, and mouse monoclonal anti-GAPDH antibody (sc-47724, Santa Cruz Biotechnology, Santa Cruz, CA) at the same dilution. The membranes were then washed five times for 5 min with PBS containing 0.1% Tween 20, followed by a 1 h incubation in blocking buffer including two infrared-dye labeled secondary antibodies at 1:10,000 dilution: goat anti-rabbit IR 800 and donkey anti-mouse IR 680 (LI-COR, Lincoln, NE, USA). Then, the membranes were subsequently washed five times and scanned for detecting protein signals with the Odyssey infrared imaging system (LI-COR, Lincoln, NE, USA). For quantitative measurement, the spots corresponding to protein were analyzed with ImageJ-NIH Image Processing Software (https://imagej.nih.gov/ij/).

The antibodies used for both, IHC and WB, does not detect the mutant truncated parafibromin.

We also assessed the expression levels of both miR-155 and miR-664 in PC tissue. To perform these assays, the cDNA was prepared from 240 ng of total DNA-free RNA, using a miScript II RT Kit (QIAGEN, Hilden, Germany) as recommended by the manufacturers. Real-time qRT-PCR analysis was performed using miScript SYBR Green PCR Kit (QIAGEN, Hilden, Germany), utilizing 12 ng of cDNA and specific forward primers, Hs_miR-155_2 and Hs_miR-664_1 miScript Primer Assay (QIAGEN, Hilden, Germany). Conditions for real-time qRT-PCR were: 95°C for 15 min, followed by 40 cycles of 94°C for 15 s, 55°C for 30 s, and 70°C for 30 s. Relative quantification was calculated through the $2^{-\Delta\Delta ct}$ method, and normalized by using *RNU-6B* gene.

Statistical analysis

All experiments were repeated three times and results were expressed as means ± standard deviation. Wilcoxon signed-rank test was used to estimate significant differences, and a p-value <0.05 was considered as statistically significant. All analyses were performed using the SPSS18 software package (IBM, Florence, Italy).

Written informed consent was obtained from the patient for the collection of biologic samples and analysis of clinical biologic data for this case report. The study was approved by the Local Ethical Committee of AOU-Careggi, Florence (Italy) for human studies (Rif. n. 12599_bio). Finally, this study was conducted in accordance with the principles of the Declaration of Helsinki.

Results

Sanger sequencing analysis of the entire coding sequence and splice sites of *CDC73* gene revealed a novel heterozygous germline deletion of one nucleotide

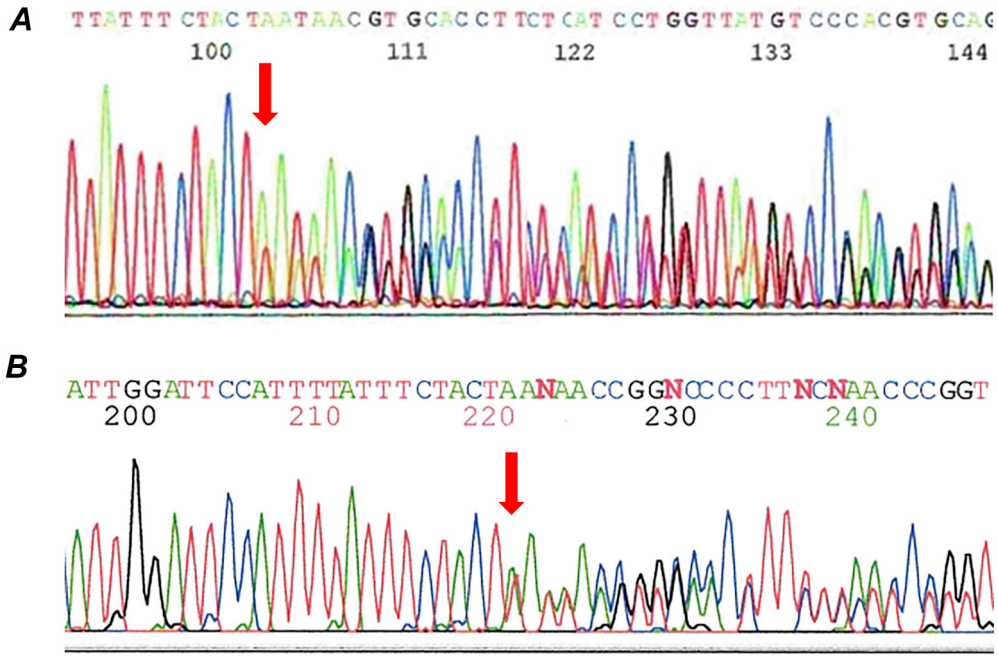

Fig. 2 Mutation of *CDC73* gene. A, DNA *CDC73* gene sequencing electropherogram shows novel germline deletion of a T (red arrow) in one allele at nucleotide 191/192, creating a frameshift in the gene structure. B, mRNA *CDC73* gene sequencing electropherogram showing the same mutation revealed in DNA *CDC73* gene.

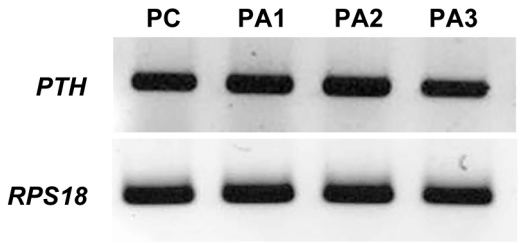

Fig. 3 Semiquantitative RT-PCR analysis to evaluate the *PTH* gene expression. PC tissue expresses the mRNA of *PTH* gene. This result shows that this tumor tissue had maintained its endocrine differentiated status. PC, parathyroid carcinoma; PA1-2-3, parathyroid adenoma control tissues.

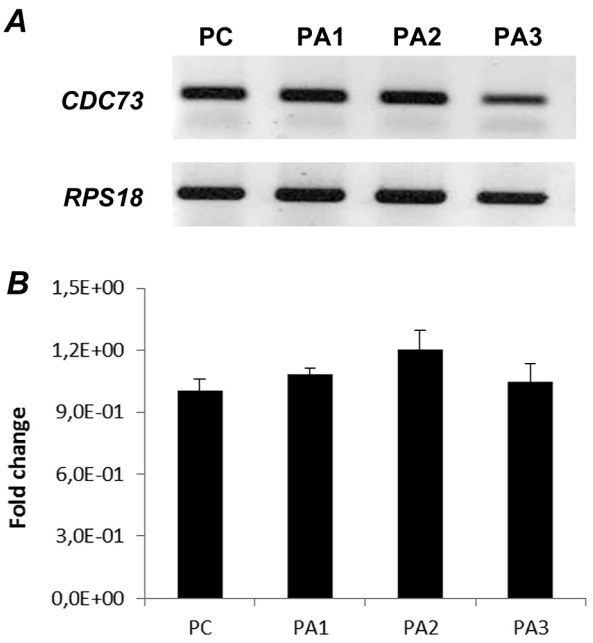

Fig. 4 Analysis of *CDC73* gene expression. Both, semi-quantitative RT-PCR (A) and real-time qRT-PCR (B) analysis do not show significant differences in *CDC73* gene expression levels between PC tissue and PAs control tissues. PC, parathyroid carcinoma; PA1-2-3, parathyroid adenoma control tissues.

in exon 2, c.191-192 delT, present in both PBL and PC tissue (Fig. 2A). No other mutation was found in the *CDC73* gene. This deletion is predicted to introduce a premature stop codon at position 108 (p.L64Lfs*44). The mutation is novel since it has not been reported in Ensembl (www.ensembl.org), in the 1000 Genomes (www.1000genomes.org/), nor Human Gene Mutation Database (www.biobase-international.com/product/hgmd).

CDC73 mRNA sequence analysis was carried out using cDNA obtained from total RNA of the PC tissue, by reverse transcription reaction. Also in this case the same heterozygous deletion founded in PBL and PC tissue, was detected (Fig. 2B).

Gene expression analysis of PC tissue showed the presence of *PTH* mRNA, with levels comparable to those found in PA control tissues (Fig. 3). The results of both RT-PCR (Fig. 4A) and real-time qRT-PCR analysis (Fig. 4B), performed to evaluate *CDC73* gene expression levels, showed that there were no significant differences in gene expression levels between PC and PA control tissues.

At IHC, almost 100% of cells in healthy parathyroid tissue of HPT-JT patient displayed strong nuclear immunoreactivity for parafibromin (Fig. 5A), whereas only isolated tumor cell nuclei were weakly stained (Fig. 5B). Ki-67 proliferative index was 10% (data not shown). These findings, along with the results of histologic analyses, were consistent with PC.

WB assay showed that the levels of parafibromin in PC tissue were markedly lower when compared with PA control tissues (Fig. 6A). Additionally, quantitative measurement of protein spots demonstrated that parafibromin expression levels in PC tissue were lower when

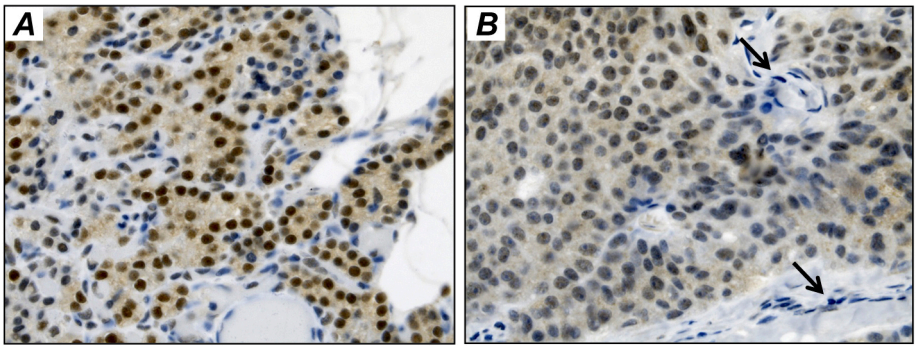

Fig. 5 Immunostaining of parafibromin. Strong nuclear immunoreactivity in the normal parathyroid tissue (A), while a high decrease of parafibromin staining was observed in PC tissue (–85%) (B). Arrows point to nuclear staining of endothelial cells (400× original magnification).

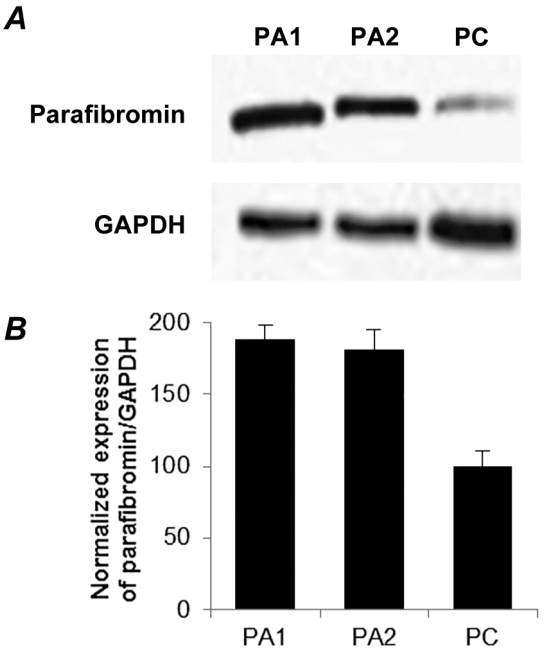

Fig. 6 Analysis of parafibromin expression. Western blotting (A) and histogram (B) showing lower parafibromin expression levels in PC than PA control tissues. PC, parathyroid carcinoma tissue; PA1-2, parathyroid adenoma control tissues. Wilcoxon signed-rank test was performed for statistical analysis. * = $p < 0.05$

compared with PA control tissues, in line with immunohistochemical findings (Fig. 6B).

miRs expression analysis in the PC tissue showed that there were no significant differences in expression levels of miR-155 and miR-664, when compared with PA control tissues (Fig. 7).

Discussion

The HPT-JT syndrome is a rare endocrine disease described for the first time in 1971 [26]. Since 1990, this syndrome has been recognized as a clinically and genetically distinct disease [27], an autosomal dominant disorder characterized by the occurrence of parathyroid neoplasia and osteofibroma. In particular, HPT-JT patients have a high risk of developing PCs, in fact 15% of the PTs are malignant [2]. In 2002, the disease-causing gene *CDC73* was mapped at chromosome 1q31.2 [4].

It has been estimated that about 80% of HPT-JT patients harbor an inactivating mutation in *CDC73* gene. Approximately 70% of all mutations occurring in the *CDC73* gene were located in exons 1, 2 and 7. Almost 50% of these mutations were frameshift deletions or insertions, 29% nonsense mutations, 6% splice site mutations and 2% in-frame deletions or insertions. Moreover, over 80% of these mutations were predicted to cause premature protein truncation [28]. Finally, approximately 70% of PC patients show somatic LOH of *CDC73* gene [15]. This is consistent with its tumor suppressor gene role described in the Knudson's "two hit" model for inherited cancer [14].

Malignant parathyroid tumors are rare endocrine and highly aggressive malignancies, accounting for less than 1% of PHPT cases [29]. The first clinical manifestation is hypercalcemia due to excessive PTH secretion, which in turn can cause organ damage, bone disease and renal failure. Therefore, early diagnosis of this neoplasia is imperative. Unfortunately, it is frequently clinically and histologically difficult to distinguish PCs from other PTs. Even the combined use of the most common genetic (*i.e. CDC73* gene) and biochemical markers (*i.e.* parafibromin and Ki-67) does not always lead to the correct diagnosis. Usually, diagnosis of PC is supported by the presence of an unequivocally invasive growth pattern or metastases [30].

We have presented the case of a patient with severe PHPT, suspected on the basis of hypercalcemia and associated OFM. The diagnosis of HPT-JT syndrome was

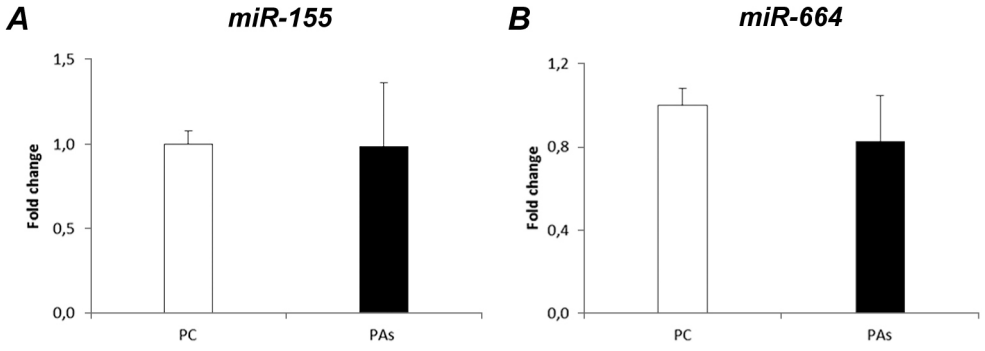

Fig. 7 Analysis of miRs expression. No significant differences in expression levels of miR-155 (A) and miR-664 (B), between PC and PAs tissues. PC, parathyroid carcinoma; PAs, parathyroid adenoma control tissues.

reached by genetic analysis of the *CDC73* gene mutations, with identification of a novel heterozygous germline mutation, c.191-192 delT, predicted to introduce a premature stop codon at position 108 (p.L64Lfs*44). PC was diagnosed after pathologic examination. Indeed, the tissue specimen showed invasive growth pattern, loss of parafibromin expression, and Ki-67 proliferation index at 10%. The reduction in parafibromin expression in PC tissue was also confirmed by WB assay.

However, these results were not consistent with data from *CDC73* gene sequencing analysis of DNA and total RNA obtained from PC tissue. Indeed, these genetic tests revealed a single heterozygous mutation, c.191-192 delT, previously detected in constitutional DNA. The absence of LOH in the parathyroid cancer cells is compatible with the maintenance of a wild type allele of the *CDC73* gene capable of encoding a functioning parafibromin protein. Hence, a decrease of parafibromin expression levels no less than 50% would have been expected compared with the healthy tissues.

One possible explanation for this discrepancy could be an inhibitor transcription mechanism of the *CDC73* gene, resulting in a reduction of more than 50% of the parafibromin protein translation. However, gene expression data showed no differences in *CDC73* mRNA expression levels in PC and control parathyroid tissues.

How can PC cells expressing a wild type allele of the *CDC73* gene and normal mRNA levels of this gene manifest decreased parafibromin protein levels by over 50% (80–90%)? We suggest that a post-transcriptional mechanism of gene silencing could play a role in determining wild type *CDC73* gene allele inactivation.

MicroRNAs, short endogenously expressed single-strand noncoding RNAs, could be one explanation. They act as negative regulators of gene expression by increasing or degrading mRNAs target and/or decreasing translational but not modifying transcription levels [16, 17]. Overall, this epigenetic mechanism seems to adequately explain our data. Over the last few years, some authors have reported miRs dysregulated expression in PC when compared with non-malignant PT tissue [19-22]. However, none of these reported miRs had *CDC73* mRNA as a putative target. To date, only two studies have identified specific miRs, miR-155 and miR-664, as responsible for downregulating *CDC73* gene expression, in oral squamous cell carcinoma [23] and MEN1 parathyroid adenoma [24], respectively. Consequently, we aimed to verify if these two miRs, miR-155 and miR-664, were dysregulated in our PC tissue cells. Our data failed to find any expression differences in either of these two miRs in PC tissue with respect to PA control tissues, confirming the data published to date. Analysis of the entire miRs with next generation sequencing techniques could be useful to understand the possible molecules involved in post-transcriptional regulation of *CDC73* gene in this clinical case.

In conclusion, we have reported the case of a HPT-JT patient, affected with PC and harboring a heterozygous germinal mutation in the *CDC73* gene. Although *CDC73* gene expression levels were normal in PC tissue, parafibromin expression was reduced by 90%. To explain these inconsistencies we hypothesize miRs-induced *CDC73* wild type allele silencing.

To date, few investigations have looked into this field, but further studies are recommended to both clarify the role of this important epigenetic gene expression regulatory mechanism in PC, and increase our knowledge of the molecular mechanisms of PC progression. Finally, knowing the specific miRs profile expression of carcinomas could provide a further useful tool for reaching a more accurate and early diagnosis of this aggressive disorder.

Acknowledgements

This work was supported by unrestricted grants from Fondazione Ente Cassa di Risparmio di Firenze and from Fondazione F.I.R.M.O. Raffaella Becagli (to M. L. Brandi).

Declaration of Interest

The Authors confirm that there are no known conflicts of interest associated with this publication and no significant financial support for this study could have influenced its outcome.

References

1. Marx SJ (2000) Hyperparathyroid and hypoparathyroid disorders. *N Engl J Med* 343: 1863–1875.
2. Chen JD, Morrison C, Zhang C, Kahnoski K, Carpten JD, *et al.* (2003) Hyperparathyroidism-jaw tumour syndrome. *J Intern Med* 253: 634–642.
3. Hobbs MR, Rosen IB, Jackson CE (2002) Revised 14.7-cM locus for the hyperparathyroidism-jaw tumor syndrome gene, HRPT2. *Am J Hum Genet* 70: 1376–1377.
4. Carpten JD, Robbins CM, Villablanca A, Forsberg L, Presciuttini S, *et al.* (2002) HRPT2, encoding parafibromin, is mutated in hyperparathyroidism-jaw tumor syndrome. *Nat Genet* 32: 676–680.
5. Bradley KJ, Hobbs MR, Buley ID, Carpten JD, Cavaco BM, *et al.* (2005) Uterine tumours are a phenotypic

manifestation of the hyperparathyroidism-jaw tumour syndrome. *J Intern Med* 257: 18–26.
6. Newey PJ, Bowl MR, Thakker RV (2009) Parafibromin–functional insights. *J Intern Med* 266: 84–98.
7. Bradley KJ, Cavaco BM, Bowl MR, Harding B, Cranston T, *et al.* (2006) Parafibromin mutations in hereditary hyperparathyroid syndromes and parathyroid tumors. *Clin Endocrinol (Oxf)* 64: 299–306.
8. Yart A, Gstaiger M, Wirbelauer C, Pecnik M, Anastasiou D, *et al.* (2005) The HRPT2 tumor suppressor gene product parafibromin associates with human PAF1 and RNA polymerase II. *Mol Cell Biol* 25: 5052–5060.
9. Mosimann C, Hausmann G, Basler K (2006) Parafibromin/Hyrax activatesWNT/Wg target gene transcription by direct association with bcatenin/Armadillo. *Cell* 125: 327–341.
10. Mosimann C, Hausmann G, Basler K (2009) The role of Parafibromin/Hyrax as a nuclear Gli/Ci-interacting protein in Hedgehog target gene control. *Mech Dev* 126: 394–405.
11. Zhang C, Kong D, Tan MH, Pappas DL Jr, Wang PF, *et al.* (2006) Parafibromin inhibits cancer cell growth and causes G1 phase arrest. *Biochem Biophys Res Commun* 350: 17–24.
12. Lin L, Zhang JH, Panicker LM, Simonds WF (2008) The parafibromin tumor suppressor protein inhibits cell proliferation by repression of the c-myc proto-oncogene. *Proc Natl Acad Sci U S A* 105: 17420–17425.
13. Woodard GE, Lin L, Zhang JH, Agarwal SK, Marx SJ, *et al.* (2005) Parafibromin, product of the hyperparathyroidism-jaw tumor syndrome gene HRPT2, regulates cyclin D1/PRAD1 expression. *Oncogene* 24: 1272–1276.
14. Knudson AG Jr (1971) Mutation and cancer: statistical study of retinoblastoma. *Proc Natl Acad Sci U S A* 68: 820–823.
15. Gill AJ (2014) Understanding the genetic basis of parathyroid carcinoma. *Endocr Pathol* 25: 30–34.
16. Croce CM, Calin GA (2005) miRNAs, cancer, and stem cell division. *Cell* 122: 6–7.
17. Iorio MV, Croce CM (2009) MicroRNAs in cancer: small molecules with a huge impact. *J Clin Oncol* 27: 5848–5856.
18. Bartel DP (2004) MicroRNAs: genomics, biogenesis, mechanism, and function. *Cell* 116: 281–297.
19. Corbetta S, Vaira V, Guarnieri V, Scillitani A, Eller-Vainicher C, *et al.* (2010) Differential expression of microRNAs in human parathyroid carcinomas compared with normal parathyroid tissue. *Endocr Relat Cancer* 17: 135–146.
20. Rahbari R, Holloway AK, He M, Khanafshar E, Clark OH, *et al.* (2011) Identification of differentially expressed microRNA in parathyroid tumors. *Ann Surg Oncol* 18: 1158–1165.
21. Vaira V, Faversani A, Dohi T, Montorsi M, Augello C, *et al.* (2012) miR-296 regulation of a cell polarity-cell plasticity module controls tumor progression. *Oncogene* 31: 27–38.
22. Vaira V, Elli F, Forno I, Guarnieri V, Verdelli C, *et al.* (2012) The microRNA cluster C19MC is deregulated in parathyroid tumours. *J Mol Endocrinol* 49: 115–124.
23. Rather MI, Nagashri MN, Swamy SS, Gopinath KS, Kumar A (2013) Oncogenic microRNA-155 down-regulates tumor suppressor CDC73 and promotes oral squamous cell carcinoma cell proliferation: implications for cancer therapeutics. *J Biol Chem* 288: 608–618.
24. Luzi E, Ciuffi S, Marini F, Mavilia C, Galli G, *et al.* (2017) Analysis of differentially expressed microRNAs in MEN1 parathyroid adenomas. *Am J Transl Res* 9: 1743–1753.
25. Costa-Guda J, Imanishi Y, Palanisamy N, Kawamata N, Koeffler PH, *et al.* (2013) Allelic imbalance in sporadic parathyroid carcinoma and evidence for its *de novo* origins. *Endocrine* 44: 489–495.
26. Kennett S, Pollick H (1971) Jaw lesions in familial hyperparathyroidism. *Oral Surg Oral Med Oral Pathol* 31: 502–510.
27. Jackson CE, Norum RA, Boyd SB, Talpos GB, Wilson SD, *et al.* (1990) Hereditary hyperparathyroidism and multiple ossifying jaw fibromas: a clinically and genetically distinct syndrome. *Surgery* 108: 1006–1012.
28. Newey PJ, Bowl MR, Cranston T, Thakker RV (2010) Cell division cycle protein 73 homolog (CDC73) mutations in the hyperparathyroidism-jaw tumor syndrome (HPT-JT) and parathyroid tumors. *Hum Mutat* 31: 295–307.
29. Marcocci C, Cetani F, Rubin MR, Silverberg SJ, Pinchera A, *et al.* (2008) Parathyroid carcinoma. *J Bone Miner Res* 23: 1869–1880.
30. DeLellis RA, Williams ED (2004) Tumours of the thyroid and parathyroid. In: DeLellis RA, Lioyd RV, Heitz PU, Eng C (Eds) WHO Classification of Tumours. Pathology and Genetics of Tumours of Endocrine Organs (3rd). IARC Press, Lyon: 49–133.